• Clinical Research •

Clinical characteristics and prognosis of solitary punctate chorioretinitis in Chinese patients

Ning-Xi Hong, Wei-Xin Zheng, Ming-Zhi Su, Fang Zheng, Pan-Pan Ye

Eye Center of Second Affiliated Hospital, Zhejiang Provincial Key Laboratory of Ophthalmology, Zhejiang Provincial Clinical Research Center for Eye Diseases, Zhejiang Provincial Engineering Institute on Eye Diseases, School of Medicine, Zhejiang University, Hangzhou 310009, Zhejiang Province, China

Co-first Authors: Ning-Xi Hong and Wei-Xin Zheng

Correspondence to: Pan-Pan Ye. Eye Center of Second Affiliated Hospital, Zhejiang Provincial Key Laboratory of Ophthalmology, Zhejiang Provincial Clinical Research Center for Eye Diseases, Zhejiang Provincial Engineering Institute on Eye Diseases, School of Medicine, Zhejiang University, Hangzhou 310009, Zhejiang Province, China. yepanpan@zju.edu.cn

Received: 2025-03-06 Accepted: 2026-01-05

Abstract

● **AIM:** To describe a case series of solitary punctate chorioretinitis (SPC), a subtype of punctate inner choroidopathy (PIC) characterized by solitary macular lesions.

● **METHODS:** This retrospective, consecutive case series included patients diagnosed with SPC over a 5-year period, all of whom had a minimum follow-up of 6mo. Baseline and multimodal imaging data were analyzed to assess clinical presentations and prognosis.

● **RESULTS:** All patients (*n*=17) were Chinese and myopic, with a female predominance (12/17, 70.6%). The mean age was 31y (range, 18–42y). The median refractive error of the affected eyes was -4.6 diopters (D; range, -14.5 to -0.75 D). Ophthalmoscopically, the lesions presented as solitary, yellow-white dots in the macula. On fundus fluorescein angiography (FFA), most lesions (15/17, 88.2%) appeared hyperfluorescent, with slight leakage observed in 3 cases (17.6%). Indocyanine green angiography (ICGA) revealed hypofluorescence in nearly all cases (16/17, 94.1%). Following a three-month course of oral glucocorticoids, most lesions (11/17, 64.7%) showed reduction or resolution. During follow-up, five patients (29.4%) developed secondary macular neovascularization (MNV), indicating a more severe disease course. Recurrences were observed in six patients. At the final visit, focal choroidal excavation was present in four patients (23.5%).

● **CONCLUSION:** SPC is a rare subtype of PIC, characterized by a favorable prognosis, although late recurrences are possible. Accurate diagnosis necessitates differentiating it from MNV. Early intervention with oral glucocorticoids appears to be an effective therapeutic strategy.

● **KEYWORDS:** solitary punctate chorioretinitis; punctate inner choroidopathy; multimodal imaging

DOI:10.18240/ijo.2026.07.12

Citation: Hong NX, Zheng WX, Su MZ, Zheng F, Ye PP. Clinical characteristics and prognosis of solitary punctate chorioretinitis in Chinese patients. *Int J Ophthalmol* 2026;19(7):1316-1324

INTRODUCTION

Punctate inner choroidopathy (PIC) is an idiopathic inflammatory condition that predominantly affects young, myopic women[1]. It is characterized by multiple lesions at the level of the retinal pigment epithelium (RPE) and inner choroid, typically located in the posterior pole. Notably, these lesions often occur in the absence of anterior chamber or vitreous inflammation[2-3]. While PIC is generally self-limiting with a favorable prognosis, a significant complication is the development of inflammatory macular neovascularization (MNV), which can lead to severe vision loss. The reported incidence of inflammatory MNV secondary to PIC is as high as 63%[4].

The etiology and pathogenesis of PIC remain incompletely understood. As a member of the white dot syndromes, PIC is hypothesized to be an autoimmune disorder that develops in genetically susceptible individuals following an environmental trigger, such as infection, immunization, or stress[5-6]. Jampol and Becker[7] proposed that an unknown insult may initiate an immune response against antigens in the outer retina or inner choroid, leading to the development of PIC.

Recent observations have identified a distinct clinical phenotype characterized by a solitary, yellow-white lesion at the level of the RPE and inner choroid. This entity was recently proposed as a novel subtype of PIC and is formally termed

solitary punctate chorioretinitis (SPC)[8]. To date, few reports have focused on SPC[9]. This study collects a series of SPC cases to report their clinical features and multimodal imaging findings, thereby enhancing the understanding of this disease and clarifying its distinction from classic PIC.

PARTICIPANTS AND METHODS

Ethics Approval This retrospective observational study was approved by the Institutional Review Board of the Eye Center, The Second Affiliated Hospital, Zhejiang University School of Medicine (Approval No.2024-0621). The study adhered to the tenets of the Declaration of Helsinki and was conducted at the aforementioned institution.

Demography and Baseline Characteristics We enrolled patients diagnosed with SPC between January 2019 and January 2024. The diagnosis of SPC was established based on a combination of characteristic clinical presentation and a comprehensive exclusionary workup. The defining clinical feature was the presence of a solitary, yellow-white macular lesion located at the level of the RPE and inner choroid, as confirmed by multimodal imaging. To rule out systemic infections and other forms of chorioretinitis, all patients underwent a baseline systemic evaluation, including chest X-ray and serological testing. For patients where clinical indication warranted further investigation, additional tests were performed. These extended investigations comprised a differential blood count, erythrocyte sedimentation rate, C-reactive protein, anti-streptococcal hemolysin O, rheumatoid factor, antinuclear antibodies, anti-neutrophil cytoplasmic antibodies, a tuberculin skin test, and serologic testing for Toxoplasma gondii (immunoglobulin M, IgM), syphilis, human immunodeficiency virus (HIV), and Bartonella henselae[10].

Diagnostic Criteria The diagnosis of SPC was established based on characteristic findings from a standardized multimodal imaging protocol. Key diagnostic criteria included the following features. Fundus photography documented a solitary, punctate, yellow-white lesion located at the level of the outer retina and choroid in the macular area. On fundus fluorescein angiography (FFA), active lesions typically demonstrated early hyperfluorescence with late-phase leakage or staining. Indocyanine green angiography (ICGA) consistently revealed hypofluorescence throughout all phases. Swept-source optical coherence tomography (SS-OCT) in the active stage showed a solitary, moderately to hyper-reflective, heterogeneous lesion disrupting the outer retinal layers with poorly defined boundaries[11]. Furthermore, the development of MNV, when present, was identified on optical coherence tomography angiography (OCTA) as a distinct neovascular network at the level of the outer retina[12]. The assessment of lesion activity was primarily based on longitudinal morphological changes observed on SS-OCT. Findings from ancillary multimodal imaging, including fundus autofluorescence (FAF), fluorescein angiography (FA), and ICGA, provided supportive diagnostic information but were not used as formal criteria for staging.

Multimodal Imaging Data At each follow-up visit, patients underwent a comprehensive ophthalmic examination starting from baseline. This included best-corrected visual acuity (BCVA) testing using the Early Treatment Diabetic Retinopathy Study (ETDRS) chart, slit-lamp examination (HAAG-STREIT BQ900, Switzerland), intraocular pressure measurement with a non-contact tonometer (NIDEK NT-510, Japan), fundus photography, and optical coherence tomography (OCT). FAF imaging was performed at the initial visit. FFA and ICGA were conducted during both the initial and final assessments. Multimodal imaging features were documented and analyzed using the following devices: color fundus photography (Optos UWF, UK; Zeiss fundus camera, Germany), FAF (Optos UWF, UK), OCT, OCTA (Intalight 150° ultra-wide angle OCT, China), as well as FFA and ICGA (Heidelberg Engineering, Germany).

All lesions were quantitatively assessed using a VG200D OCT system (SVision Imaging, China). The imaging protocol consisted of 12 high-resolution radial B-scans (6 mm in length) centered on the lesion, as well as 6×6 mm^2 volumetric scans (512×512 A-scans) for lesion diameter measurement. Lesion diameter was measured on en face OCT images using the built-in caliper tool of the SVision OCT software (v3.2). Lesion height was quantified on cross-sectional B-scans obtained with enhanced-depth imaging (EDI) mode as the vertical distance from Bruch's membrane (BRM) to the inner surface of the lesion. Lesions typically appeared as semicircular nodules of moderate to high reflectivity beneath the central fovea, projecting toward the outer retina or inner choroid. Changes in nodule size on serial OCT examinations were analyzed to determine disease activity. Subfoveal choroidal thickness (SFCT) was also systematically measured.

To ensure consistency in image interpretation, all OCT, OCTA, FFA, and ICGA images were evaluated by two independent retinal specialists who were masked to treatment allocation and clinical outcomes. Any discrepancies between their assessments were resolved through adjudication by a third senior ophthalmologist, also masked to patient information.

Statistical Analysis All statistical analyses were conducted with SPSS 27.0. Categorical variables are presented as frequencies and percentages (*n*, %). For these data, intra-group comparisons were made using the McNemar's test, while inter-group comparisons were assessed with the Chi-square test or Fisher's exact test, as appropriate. Continuous data were assessed for normality. Normally distributed data are expressed as mean±SD and were compared within groups using a paired

Table 1 Patient-specific characteristics in 17 patients with SPC

Items	Sex	Age (y)	Symptoms	Affected eye	Baseline spherical equivalent (D)	BCVA at baseline (Snellen scores)	Treatment	BCVA at the final visit	Follow-up time (mo)	Events (regression /FCE/ recurrence/MNV)
1	F	23	Blurred vision	OS	-4.75	20/50	Oral glucocorticoids	20/20	44	Regression
2	F	32	Blurred vision	OS	-7.00	20/100	Oral glucocorticoids	20/20	10	Regression
3	F	32	Blurred vision, metamorphosia	OD	-6.50	20/25	Oral glucocorticoids	20/20	68	Regression
4	F	39	Scotoma	OS	-4.25	20/200	Oral glucocorticoids	20/25	6	Regression
5	M	35	Blurred vision	OS	-0.75	20/25	Oral glucocorticoids	20/33	6	Regression
6	M	29	Metamorphosia	OD	-1.50	20/20	Oral glucocorticoids	20/20	6	Regression
7	F	37	Blurred vision	OD	-6.00	20/20	Oral glucocorticoids	20/20	6	Regression
8	F	31	Blurred vision	OD	-3.50	20/66	Oral glucocorticoids	20/20	42	Formation of FCE
9	F	33	Blurred vision, metamorphosia	OD	-1.00	20/50	Oral glucocorticoids	20/40	24	Formation of FCE
10	F	28	Blurred vision, metamorphosia	OS	-2.75	20/40	Oral glucocorticoids	20/20	6	Formation of FCE
11	M	32	Blurred vision	OS	-2.50	20/200	Oral glucocorticoids	20/100	15	Recurrence, formation of FCE
12	M	18	Blurred vision	OD	-5.25	20/100	Oral glucocorticoids	20/25	6	Recurrence
13	M	31	Blurred vision	OS	-2.50	20/200	Oral glucocorticoids and anti-VEGF	20/66	14	Recurrence, development of MNV
14	F	25	Metamorphosia	OS	-4.25	20/25	Oral glucocorticoids and anti-VEGF	20/20	26	Recurrence, development of MNV
15	F	42	Metamorphosia	OS	-14.5	20/100	Oral glucocorticoids and anti-VEGF	20/20	30	Recurrence, development of MNV
16	F	28	Scotoma	OD	-3.75	20/40	Oral glucocorticoids And anti-VEGF	20/25	25	Recurrence, development of MNV
17	F	27	Blurred vision, metamorphosia	OD	-7.5	20/40	Oral glucocorticoids and anti-VEGF	20/20	7	Development of MNV

SPC: Solitary punctate chorioretinitis; M: Male; F: Female; OD: Oculus dexter; OS: Oculus sinister; BCVA: Best-corrected visual acuity; anti-VEGF: Anti-vascular endothelial growth factor; MNV: Macular neovascularization; FCE: Focal choroidal excavation. Patients are grouped and ordered by the primary clinical event observed during follow-up.

t-test and between groups using an independent samples *t*-test. Non-normally distributed data are summarized as median with interquartile range; the Wilcoxon signed-rank test was used for intra-group comparisons, and the Mann-Whitney *U* test for inter-group comparisons. *P*-values less than 0.05 were considered statistically significant.

RESULTS

Basic Characteristics This study included 17 eyes from 17 patients diagnosed with SPC. All patients completed a comprehensive exclusion workup prior to enrollment. The cohort consisted of 12 females (70.6%) and 5 males, with a median age of 31y (range: 18–42). All patients were myopic, with a median spherical equivalent of -4.6 diopters (D; range: -14.5 to -0.75 D) in the affected eyes. Disease presentation was unilateral in all cases. The most common initial symptoms were blurred vision (70.6%), metamorphopsia (41.2%), and scotoma (11.8%). Only two patients reported a preceding common cold before onset. On multimodal imaging, all lesions appeared as solitary yellowish-white foci located at the level of the outer retina, RPE, and inner choroid in the macular region (Table 1).

All patients were treated with oral glucocorticoids. During the 12-month follow-up period following the initial visit, five patients (5/17, 29.4%) developed MNV and received adjunctive anti-VEGF therapy. The median BCVA was 20/50. Following treatment, the majority of patients (14/17, 82.4%) demonstrated significant visual improvement, with a mean gain of 18 ETDRS letters. Sequential OCT and fundus photography revealed gradual lesion resolution in 11 patients (11/17, 64.7%) within 3mo after treatment initiation. However, six patients experienced disease recurrence following glucocorticoid discontinuation, which was frequently associated with systemic triggers such as fatigue or upper respiratory infection. Throughout the follow-up period, five patients developed MNV, and four patients (4/17, 23.5%) exhibited focal choroidal excavation (FCE) at the final visit. The median follow-up duration was 20mo (range: 6–68mo).

Among the five patients who developed MNV, the mean baseline spherical equivalent was -6.50 D. Following the diagnosis of SPC, all patients received treatment with oral corticosteroids, which were discontinued after a mean of 1mo due to subjective improvement in symptoms. MNV was first detected at a mean of 3.6mo after the initial presentation. All five patients subsequently underwent anti-VEGF therapy upon detection of MNV. The MNV regressed after a mean period of 10mo of treatment and did not recur during subsequent follow-up.

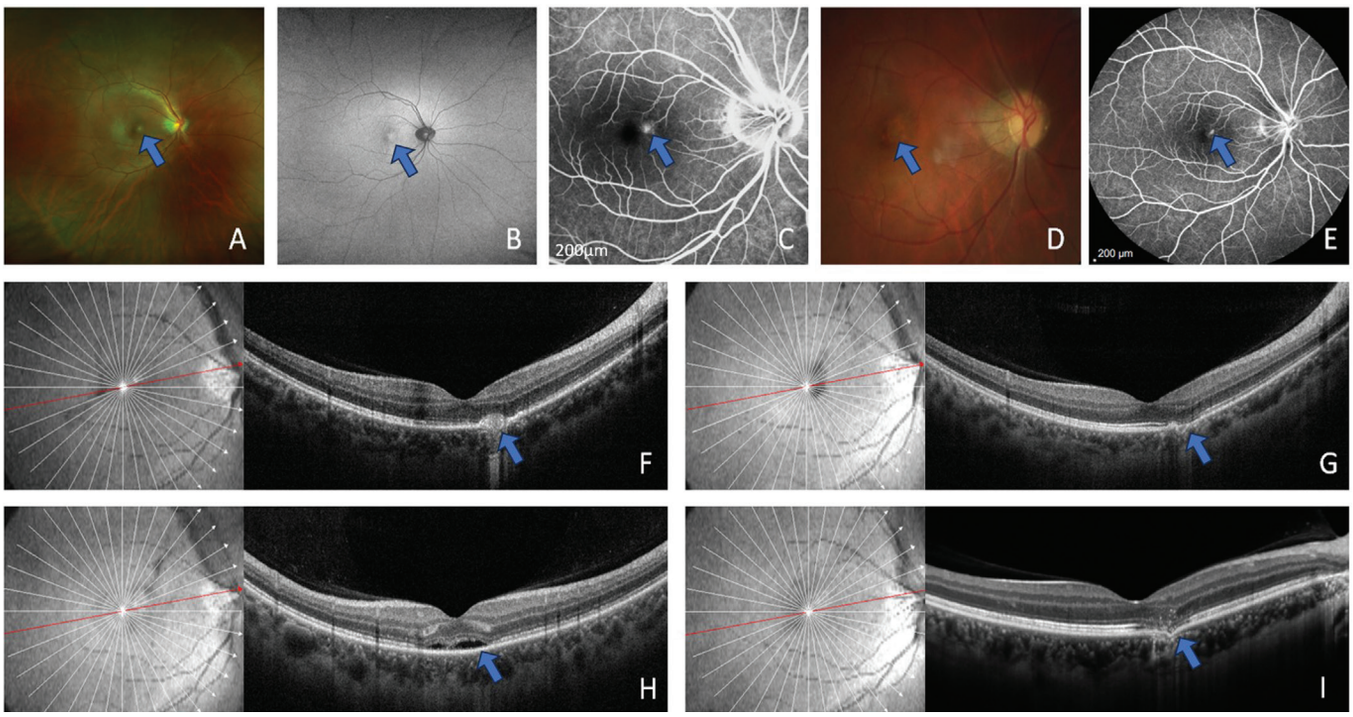

Figure 1 Sequential multimodal imaging reveals a macular lesion in patient 9 that regressed from a hyperautofluorescent punctate dot with RPE disruption to a focal choroidal excavation A-C: Fundus photography, fundus autofluorescence and FFA at the time of the initial visit of patient 9. A: A small yellow-white dot appears on the macular area; B: The lesion on the macular area was hyperautofluorescent; C: FFA shows that the lesion on the macular area was punctate hyperfluorescent, and the optic disc boundaries were unclear with vascular staining; D: Fundus photography was found at the patient's last follow-up. The follow-up time at this point was 15mo. E: FFA show window defect at late phase. The follow-up time at this point was 15mo. F: SS-OCT show discontinuity of the RPE layer and a semicircular bulge toward the out retinal layer at the time of the initial visit; G: The lesion was absorbed, and tissue was lost at the 11-month follow-up; H: OCT at the 11-month follow-up shows a focal choroidal excavation with no residual hyperreflective lesion. A hyporeflective area beneath the excavation is present. I: Focal choroidal excavation was formed on the OCT finding at the time of the last visit. FFA: Fundus fluorescein angiography; SS-OCT: Swept-source optical coherence tomography; RPE: Retinal pigment epithelium; OCT: Optical coherence tomography.

Multimodal Imaging Results SS-OCT at initial diagnosis revealed disruption of the RPE continuity in 11 patients, manifesting as semicircular elevations or protrusions toward the outer retinal or choroidal layers. During follow-up, six of these patients exhibited regression of the nodule from its apical portion toward the choroid. Concurrently, a V-shaped herniation of the outer plexiform layer and outer retinal layers was observed through the defect in the RPE and BRM. A previously established 5-stage classification system for PIC lesions, based on angiographic and electrophysiologic features, was referenced for context[13]. One patient, who already presented with stage IV manifestations at the initial visit, showed tissue detachment between the photoreceptor layer and the choroid, forming a V-shaped configuration oriented toward the choroid. Seven other patients, who presented with milder initial symptoms, demonstrated focal RPE elevation with interruption of the ellipsoid zone (Figure 1).

The treatment response was assessed by calculating the within-patient relative change for each directly measured parameter to avoid biases associated with comparing uncorrected absolute values across eyes (Table 2). Both the diameter and height of the lesions demonstrated significant regression. The mean relative reduction in lesion diameter was 66.3%. Similarly, lesion height decreased by a mean of 60.4%. Concurrently, SFCT showed significant thinning, with a mean relative reduction of 15.5%[14]. Five patients developed secondary MNV during follow-up and received anti-VEGF therapy. MNV lesions regressed in all five cases, with complete resolution and absence of scarring in three patients. Four patients developed FCE[15], while the remaining patients showed RPE repair (Table 2).

OCTA is able to observe the secondary MNV and its level clearly. In active lesion, it appeared as a network of hyperreflective vessels seen at the level of the choriocapillaris, sometimes extending into the outer retina, and accompanied by subretinal fluid (Figure 2).

OCTA provided more accurate diagnostic information than conventional OCT at the initial visit and was essential for ruling out MNV in all cases. MNV presence was not directly associated with lesion size. OCTA enabled differentiation between active inflammatory lesions and MNV in cases of

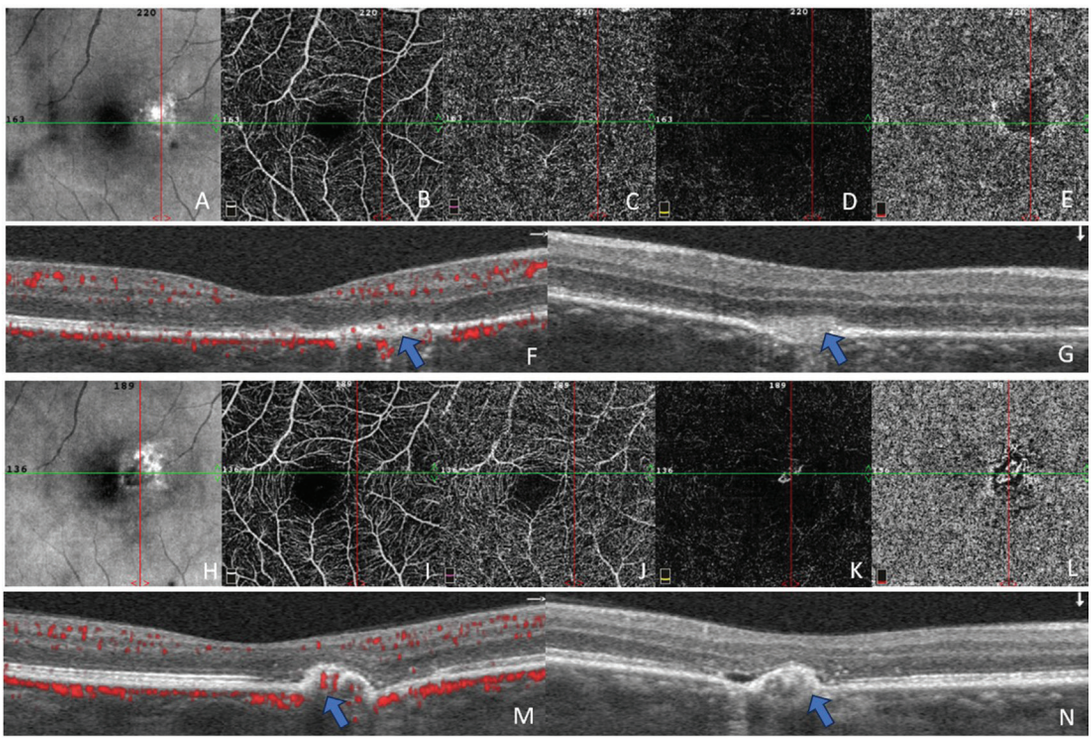

Figure 2 OCTA findings at the first visit of patient 11 (A-G) and at 15mo follow-up (H-N) No MNV was found at first visit; A: SLO; B: Superficial ILM-IPL; C: Deep IPL-OPL; D: Outer retina (OPL-BRM); E: Choriocapillaris (BRM-BRM+30 μm); F: The green line on the en face image indicates the horizontal location of the B-scan cross-section; G: The red line represents the vertical direction; H: SLO; I: Superficial ILM-IPL: J: Deep IPL-OPL; K: Outer retina (OPL-BRM); L: Choriocapillaris (BRM-BRM+30 μm); M: The green line on the en face image indicates the horizontal location of the B-scan cross-section, showing MNV; N: The red line represents the vertical direction. MNV was found at 15mo follow-up. OCTA: Optical coherence tomography angiography; MNV: Macular neovascularization; SLO: Scanning laser ophthalmoscopy; ILM: Internal limiting membrane; IPL: Inner plexiform layer; OPL: Outer plexiform layer; BRM: Bruch's membrane.

Table 2 Characterization of the lesions on multimodal imaging

Parameters	Relative changes in anatomical parameters following treatment			
	Relative change from baseline, %	Median (IQR), %	P^a	95%CI
Diameter size of lesion	-66.3±7.2	-68.3 (-71.9, -66.8)	<0.001	-70.0 to -62.6
Thickness of the lesion	-60.4±10.3	-60.3 (-68.4, -56.9)	<0.001	-65.7 to -55.2
SFCT	-15.5±4.4	-14.9 (-17.9, -11.9)	<0.001	-17.8 to -13.3
	Active stage	Regress stage		
MNV, *n* (%)	0	5/17, 29.41%		
FCE, *n* (%)	0	4/17, 23.53%		
RPE disruption, *n* (%)	17/17, 100%	7/17, 41.18%		
ELM disruption, *n* (%)	11/17, 64.71%	2/17, 11.76%		
EZ disruption, *n* (%)	16/17, 94.12%	6/17, 35.29%		

[a]The *P* value is derived from a paired *t*-test performed on the relative change percentages for each parameter, testing the null hypothesis that the mean relative change is zero. SFCT: Subfoveal choroidal thickness; IQR: Interquartile range; CI: Confidence interval; FCE: Focal choroidal excavation; RPE: Retinal pigment epithelium; ELM: External limiting membrane; EZ: Ellipsoid zone; MNV: Macular neovascularization.

SPC[16]. FFA, ICGA, and FAF were also performed during the initial evaluation. On FFA, most patients (15/17, 88.2%) exhibited punctate hyperfluorescence in the macular region during the arteriovenous phase, with mild leakage observed in three cases (3/17, 17.6%). Hyperfluorescence persisted throughout the early and late venous phases. Two patients (2/17, 11.8%) showed optic disc staining. ICGA revealed corresponding hypofluorescence in most patients (16/17, 94.1%), visible as hypoperfused choroidal lesions in both early and late phases. Two patients (2/17, 11.8%) displayed no significant abnormalities on initial fundus imaging. Among the five patients who developed secondary MNV, ICGA showed strong punctate fluorescence in the macular area with faintly visible neovascular networks.

DISCUSSION

PIC was originally reported by Watzke *et al*[1] in 1984, and numerous related studies have since been published. SPC represents a recently identified variant of PIC, characterized by a solitary punctate lesion confined to the fovea. However, published data on SPC remain scarce, and existing reports are limited by relatively short follow-up durations. The present study augments this limited literature by reporting on a larger patient cohort with an extended follow-up period.

The study cohort comprised 12 females with a median age of 31y; all patients were myopic, which aligns with the established demographic profile of PIC. The most common presenting symptoms were blurred vision and metamorphopsia. Clinical examination revealed solitary, yellowish-white macular dots in most patients, with no evidence of anterior chamber or vitreous inflammation. All patients received oral glucocorticoids, and five who developed MNV during follow-up received adjunctive anti-VEGF therapy. Following treatment, 82.4% of patients exhibited improved visual acuity at the final visit. Notably, ten patients achieved a final BCVA of 20/20, suggesting that SPC carries a favorable visual prognosis (Figure 3).

SPC represents a rare variant of PIC. Given its frequent association with myopia, SPC was initially hypothesized to represent a "lacquer crack-like chorioretinal scar"[17-18]. Lacquer cracks are characterized on OCT by discontinuities in BRM and irregularities in the RPE, and on FAF by hypoautofluorescent lines surrounded by hyperautofluorescence. These imaging features share certain similarities with those seen in SPC. In our cohort, the median refractive error was -4.6 D (range: -14.5 to -0.75 D), with 6 of 17 patients (35.3%) meeting the diagnostic criterion for high myopia (≤-6.0 D). Posterior staphyloma was observed in two patients, and lacquer cracks adjacent to the fovea were identified in one. We speculate that in genetically susceptible individuals, mechanical stress or other insults may trigger an autoimmune response against antigens in the outer retina or inner choroid, leading to the focal inflammation that characterizes SPC.

Accurate diagnosis of SPC requires more than morphological assessment alone, particularly in distinguishing it from MNV. Multimodal imaging plays a critical role in this differentiation[19]. SS-OCT effectively documents inflammatory lesion progression, especially in early stages, and has advanced our understanding of SPC. While FFA remains the gold standard for MNV detection, it can be challenging to differentiate MNV from active inflammation in SPC, as both may present as hyperfluorescence with late leakage[20]. In contrast, OCTA non-invasively visualizes blood flow, enabling direct depiction of neovascular networks and facilitating differentiation between MNV and inflammatory lesions[21-22]. MNV morphology on OCTA may further provide clues regarding lesion activity. However, detecting MNV in PIC/SPC remains difficult, as secondary MNV lesions are often too small for detailed structural assessment. Therefore, an integrated approach combining multimodal imaging with thorough clinical and demographic evaluation is essential, particularly in early disease stage[23].

Anti-VEGF therapy demonstrates limited efficacy in the early stages of SPC. In contrast, patients generally demonstrate favorable responses to glucocorticoids, with symptomatic improvement following regular administration[24]. During follow-up, BCVA typically improves, accompanied by a reduction in lesion diameter and height. In most cases, lesions gradually decrease in size and resolve within approximately three months, with progressive restoration of RPE continuity. However, some patients discontinue glucocorticoid therapy upon symptomatic relief. Notably, disease recurrence frequently occurs following treatment cessation, often triggered by identifiable factors such as physical exertion or preceding infection. A subset of patients with SPC develops MNV following recurrent inflammatory activity. The pathogenesis of myopic MNV in this context, while not fully elucidated, is thought to involve persistent inflammation. During inflammatory episodes, activated immune cells and RPE cells release pro-inflammatory cytokines that directly upregulate VEGF expression. Concurrently, inflammation-derived reactive oxygen species activate the nuclear factor (NF)-κB signaling pathway, further amplifying VEGF production and sustaining a pro-inflammatory feedback loop. This cascade ultimately compromises the structural integrity of the choroid-RPE-BRM complex, creating a permissive environment for MNV development. A notable finding in this study was that a subset of patients who developed secondary MNV maintained good BCVA. This observation, which contrasts with the typically poor prognosis associated with MNV, likely reflects the distinct pathophysiology of MNV in SPC. First, MNV in this context is predominantly type 1, and its activity is intrinsically linked to the underlying choroidal inflammation. Consequently, when the primary inflammatory disease enters remission or is controlled with immunosuppression, the driving stimulus for the MNV may resolve, allowing it to become quiescent. Second, the prompt initiation of anti-VEGF therapy upon detection of exudation can effectively suppress fluid leakage, thereby preventing chronic macular edema and irreversible photoreceptor damage. Thus, the combination of managing the fundamental inflammatory process and applying targeted anti-VEGF treatment can modify the natural history of MNV in SPC, explaining the favorable visual outcomes seen in some patients in this cohort. Accurate and timely diagnosis is therefore essential in SPC management. Early intervention

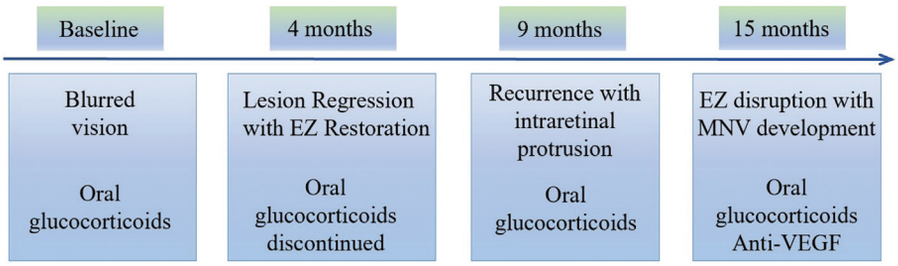

Figure 3 Therapeutic timeline for a representative patient with SPC who developed MNV The diagram illustrates the sequence of key events: symptom onset and initial diagnosis, oral glucocorticoid initiation, MNV confirmation by OCTA, subsequent anti-VEGF injections, and follow-up milestones. The timeline demonstrates the close temporal relationship between MNV diagnosis and the initiation of anti-VEGF therapy. The patient's course was representative of the overall cohort. SPC: Solitary punctate chorioretinitis; MNV: Macular neovascularization; OCTA: Optical coherence tomography angiography; VEGF: Vascular endothelial growth factor; EZ: Ellipsoid zone.

with oral glucocorticoids effectively controls inflammatory activity and mitigates disease progression. Furthermore, in cases where inflammatory damage leads to RPE breakdown and subsequent MNV formation, anti-VEGF therapy provides targeted control of neovascularization[25] (Figure 4).

Early SS-OCT imaging demonstrated an intact RPE and BRM, suggesting that structural disruption results from inflammatory activity rather than representing a primary defect. Recent OCT studies have further identified several distinctive features in affected eyes, including focal hyporeflective zones, architectural disorganization of the sublesional choroid, localized disruptions of the RPE/BRM complex, and posterior bowing of BRM[26]. Nevertheless, the precise anatomical origin of inflammation in SPC remains uncertain. It is still unclear whether the process initiates at the level of the RPE/BRM complex or within the choroid. On FFA, lesions exhibited persistent hyperfluorescence throughout the venous phase, while ICGA revealed corresponding hypofluorescence with sharper morphological delineation in the late phase[27].

While PIC carries a well-established high risk of secondary MNV[28-29], the propensity for MNV development in its solitary variant remains poorly characterized. This study provides quantitative data to address this knowledge gap. In our cohort of 17 patients, five developed MNV during follow-up. This proportion exceeds the 16.7% MNV incidence reported in the earlier SPC cohort by Zhang *et al*[4], yet remains notably lower than the reported 63% MNV risk associated with classic PIC in Chinese populations.

This study has several limitations that warrant consideration. First, its retrospective design and small sample size constrain the statistical power and preclude robust subgroup analyses. Second, the variable duration of follow-up may result in an underestimation of long-term outcomes, such as disease recurrence and MNV development. Third, as a single-center investigation involving exclusively Chinese participants, the generalizability of the findings to other ethnic or geographic populations may be limited. Additionally, the high prevalence

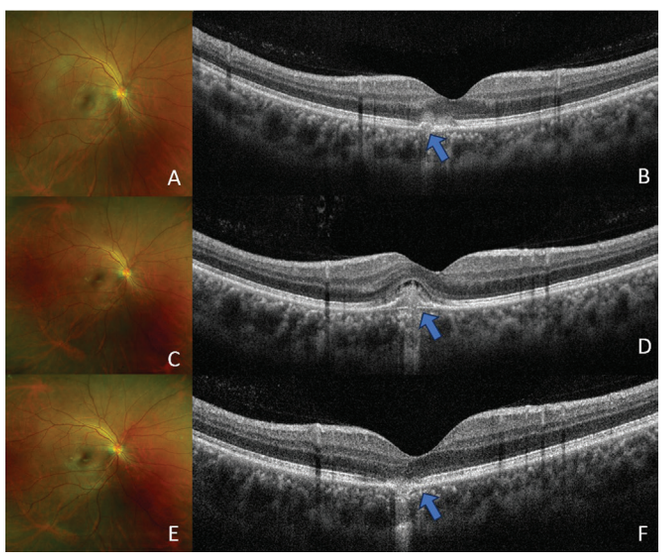

Figure 4 Over 5y follow-up of a 32-year-old female patient A: Fundus photography at the patient's initial consultation; B: OCT findings at the time of the patient's initial diagnosis, which showed a continuous break in the RPE with a semi-elliptical bulge formed by the lesion toward the inner retina; C: Fundus photography after 4y of follow-up; D: OCT findings at the time of neovascularization after 4y of follow-up; E: Fundus photography at the last follow-up; F: OCT findings at the last follow-up, when the patient's BCVA was 20/20. The continuity of RPE was still broken. OCT: Optical coherence tomography; RPE: Retinal pigment epithelium; BCVA: Best-corrected visual acuity.

of pathologic myopia in our cohort represents a potential confounder, as its imaging features may overlap with those of SPC, making it challenging to completely isolate the specific effects of the inflammatory process. Furthermore, the absence of routine baseline OCTA to exclude pre-existing MNV. Although baseline activity was determined by the absence of leakage on FA/ICGA, OCTA is more sensitive for detecting non-exudative type 1 MNV. Thus, some enrolled eyes may have had subclinical MNV, possibly affecting their initial classification and observed course. Future studies with systematic diagnostic OCTA are needed to accurately define

MNV incidence and evolution in this population. Another recognized limitation in that the reported lesion diameters were not corrected for axial length. In highly myopic eyes, this can lead to an overestimation of true size on OCT, limiting the validity of absolute cross-patient comparisons. Consequently, our analysis emphasized relative changes in lesion size over time, which are independent of magnification error. Finally, the absence of intraclass correlation coefficient (ICC) analysis for OCT image interpretation means that inter-observer variability was not formally quantified. Nevertheless, the utilization of standardized automated tools and adjudication by a senior grader likely reduces potential bias in image assessment.

In conclusion, this study presents a new subtype of PIC in Chinese patients. Although most patients had favorable prognosis, it is essential to identify active MNV in patients with SPC and provide prompt intervention[30].

ACKNOWLEDGEMENTS

Authors' Contributions: Hong NX, Zheng WX, and Su MZ wrote the main manuscript text and prepared Figures 1-4. Hong NX, Zheng WX, and Su MZ prepared data collection and statistical analysis. Zheng F performed and interpreted the specialized OCTA analysis. Ye PP designed the research, edited and revised the manuscript. All authors reviewed the result and manuscript.

Availability of Data and Materials: All data generated or analyzed during this study are included in this published article.

Foundations: Supported by Zhejiang Provincial Natural Science Foundation of China (No.LTGY24H120002); the National Natural Science Foundation of China Youth Science Fund Project (No.82201196).

Conflicts of Interest: **Hong NX,** None; **Zheng WX,** None; **Su MZ,** None; **Zheng F,** None; **Ye PP,** None.

REFERENCES

1 Watzke RC, Packer AJ, Folk JC, *et al*. Punctate inner choroidopathy. *Am J Ophthalmol* 1984;98(5):572-584.

2 Amer R, Lois N. Punctate inner choroidopathy. *Surv Ophthalmol* 2011;56(1):36-53.

3 Ahnood D, Madhusudhan S, Tsaloumas MD, *et al*. Punctate inner choroidopathy: a review. *Surv Ophthalmol* 2017;62(2):113-126.

4 Zhang XZ, Wen F, Zuo CG, *et al*. Clinical features of punctate inner choroidopathy in Chinese patients. *Retina* 2011;31(8):1680-1691.

5 Quillen DA, Davis JB, Gottlieb JL, *et al*. The white dot syndromes. *Am J Ophthalmol* 2004;137(3):538-550.

6 Kalogeropoulos D, Rahman N, Afshar F, *et al*. Punctate inner choroidopathy: a review of the current diagnostic and therapeutic approaches. *Prog Retin Eye Res* 2024;99:101235.

7 Jampol LM, Becker KG. White spot syndromes of the retina: a hypothesis based on the common genetic hypothesis of autoimmune/inflammatory disease. *Am J Ophthalmol* 2003;135(3):376-379.

8 Gan YH, He GQ, Zeng YK, *et al*. Solitary punctate chorioretinitis: a unique subtype of punctate inner choroidopathy. *Retina* 2023;43(9):1487-1495.

9 Liu C, Liu MK, Lan XY, *et al*. 91-month follow-up of solitary punctate chorioretinitis in a Chinese patient. *BMC Ophthalmol* 2024;24(1):297.

10 Gerstenblith AT, Thorne JE, Sobrin L, *et al*. Punctate inner choroidopathy. *Ophthalmology* 2007;114(6):1201-1204.e4.

11 Zheng F, Deng XF, Zhang Q, *et al*. Advances in swept-source optical coherence tomography and optical coherence tomography angiography. *Adv Ophthalmol Pract Res* 2023;3(2):67-79.

12 Shakoor A, Vitale AT. Imaging in the diagnosis and management of multifocal choroiditis and punctate inner choroidopathy. *Int Ophthalmol Clin* 2012;52(4):243-256.

13 Zhang XZ, Zuo CG, Li M, *et al*. Spectral-domain optical coherence tomographic findings at each stage of punctate inner choroidopathy. *Ophthalmology* 2013;120(12):2678-2683.

14 Kim YH, Oh J. Choroidal thickness profile in chorioretinal diseases: beyond the macula. *Front Med (Lausanne)* 2021;8:797428.

15 Verma S, Kumar V, Azad S, *et al*. Focal choroidal excavation: review of literature. *Br J Ophthalmol* 2021;105(8):1043-1048.

16 Klufas MA, O'Hearn T, Sarraf D. Optical coherence tomography angiography and widefield fundus autofluorescence in punctate inner choroidopathy. *Retinal Cases Brief Rep* 2015;9(4):323-326.

17 Herbort CP, Papadia M, Neri P. Myopia and inflammation. *J Ophthalmic Vis Res* 2011;6(4):270-283.

18 Cicinelli MV, Del Fabbro S, Ramtohul P, *et al*. Idiopathic multifocal choroiditis/punctate inner choroidopathy as a secondary inflammatory reaction to lacquer cracks: a structural and temporal analysis. *Am J Ophthalmol* 2026;282:263-276.

19 de Groot EL, ten Dam-van Loon NH, Kouwenberg CV, *et al*. Exploring imaging characteristics associated with disease activity in idiopathic multifocal choroiditis: a multimodal imaging approach. *Am J Ophthalmol* 2023;252:45-58.

20 Astroz P, Miere A, Mrejen S, *et al*. Optical coherence tomography angiography to distinguish choroidal neovascularization from macular inflammatory lesions in multifocal choroiditis. *Retina* 2018;38(2):299-309.

21 Gan YH, Zhang XZ, Su YY, *et al*. OCTA versus dye angiography for the diagnosis and evaluation of neovascularisation in punctate inner choroidopathy. *Br J Ophthalmol* 2022;106(4):547-552.

22 Levison AL, Baynes KM, Lowder CY, *et al*. Choroidal neovascularisation on optical coherence tomography angiography in punctate inner choroidopathy and multifocal choroiditis. *Br J Ophthalmol* 2017;101(5):616-622.

23 Chen CL, Cheng YZ, Zhang ZH, *et al*. The multimodal imaging features and outcomes of multifocal choroiditis/punctate inner choroidopathy lesion with multiple evanescent white dot syndrome-like features: a retrospective study. *BMC Ophthalmol* 2024;24(1):3.

24 Chen SN, Chen YL, Yang BC. Long-term outcome of zonal outer retinopathy in punctate inner choroidopathy or multifocal choroiditis. *Ocul Immunol Inflamm* 2021;29(5):865-870.

25 Wu W, Li SY, Xu HW, *et al*. Treatment of punctate inner choroidopathy with choroidal neovascularization using corticosteroid and intravitreal ranibizumab. *BioMed Res Int* 2018;2018:1585803.

26 Chen YR, Chen Q, Li XX, *et al*. RPE disruption and hyper-transmission are early signs of secondary CNV with punctate inner choroidopathy in structure-OCT. *BMC Ophthalmol* 2021;21(1):427.

27 Bouchenaki N, Cimino L, Auer C, *et al*. Assessment and classification of choroidal vasculitis in posterior uveitis using indocyanine green angiography. *Klin Monatsbl Augenheilkd* 2002;219(4):243-249.

28 Bottazzi L, Barlocci E, Sacconi R, *et al*. Choroidal neovascularization secondary to punctate inner choroidopathy vs myopia: clinical outcomes after 1-year of treatment. *Graefes Arch Clin Exp Ophthalmol* 2025;263(7):1859-1865.

29 Del Fabbro S, Perna L, Introini U, *et al*. Macular complications predict visual decline in punctate inner choroidopathy. *Ophthalmology* 2026;133(2):288-291.

30 Brown J Jr, Folk JC, Reddy CV, *et al*. Visual prognosis of multifocal choroiditis, punctate inner choroidopathy, and the diffuse subretinal fibrosis syndrome. *Ophthalmology* 1996;103(7):1100-1105.